

The Influence of Doppler Effects in HAP-OFDMA Systems

Michael Bank¹, S. Tapuchi² M. Haridim¹, Miriam Bank³, B. Hill⁴, U. Mahlab¹ J.Gavan²
¹HIT-Holon Institute of Technology, ²Sami Shamoon Engineer College, ³Hebrew
University Jerusalem, ⁴Ness Co.
bankmichael1@gmail.com

Abstract—we consider the impact of Doppler frequency shift on the Orthogonal Frequency Division Multiple Access (OFDMA) signal and Frequency Bank Signal (FBS) transmitted over High Altitude Platforms (HAPs).

Theoretical analysis and simulations show that OFDMA systems perform well when the Doppler frequency shift is smaller than 2% of carrier frequency separation. These conditions correspond to operation frequency of 2GHz and train velocities up to 120 km/h. FBS method, on the other hand, allows working under more severe Doppler effects, namely a Doppler shift of up to 6 - 8 %, hence enabling higher carrier frequency bands and higher vehicle speeds.

Keywords—OFDMA, Doppler shift, Pilot signals, FBS, HAPs, Mobile communications.

1. INTRODUCTION

Terrestrial mobile radio Communication systems are expanding increasingly and fast. However, lack of Line of Sight (LOS) propagation conditions results in shadowing and multi-path fading which limit the quality and the operation range of these systems.. The LOS conditions and operation ranges can be extended significantly using costly Geostationary (GEO) satellites at an altitude of about 36000 km [1,2] A new technique for efficient mobile radio communication systems is the High Altitude Platforms (HAPs) located in the stratosphere at an altitude of the order of 17 to 24 km ,where wind velocity is minimal, for relaying radio stations [3,4]. These HAP stations will be stabilized relative to the ground as Stratospheric Quasi Stationary Platforms (SQ-SP) due to significant progress in technology [5,6]. The performances of HAPs are in several aspects better than GEO and LEO satellites and terrestrial radio system alternatives [1]

One important future HAPS application is related to radio communications with very high speed trains or aircrafts. In these cases HAPs are significantly better than terrestrial radio due to the improved LOS propagation conditions ,much less Doppler frequency shift effects and fewer hand over events with relay stations, as shown in the scenario of figure1.The reduction in Doppler frequency shifts is due to the

relatively low transmission angles because of the HAPS altitude[7,8].

HAPs are also better than GEO satellites due to the significantly less dispersion losses and time delay. However, even for HAPs with very high speed vehicles and high carriers frequencies, required for transmission of broad band signals and fast internet, the significant Doppler frequency shift effects can deteriorate the quality of the radio link [1,7].

A multiplexing technique recommended also for the HAP radio systems is the Orthogonal Frequency Division Multiple Access (OFDMA) which provides improved frequency efficiency and reduces the Multi-Path Propagation (MPP) influence [9], However OFDMA based systems are vulnerable to poor frequency synchronization due to Doppler effects. Thus, OFDMA fails to combat the Doppler shift influence.

In addition, OFDMA requires various additional signals such as high power pilot signals, which decrease the spectral efficiency especially with limited power systems like HAPs.

In OFDMA, pilot signals may be used on the same additional carriers as in Terrestrial Digital Video Broadcasting (DVB-T and DVB-H) systems. Besides pilot signals, the OFDMA signals include additional guard intervals.

For checking Doppler Effect influence on OFDMA system an experimental assessment of received DVD-T signal quality during motion

was performed. Experiments were performed in collaboration with the Measurement Laboratory of the Israeli Communication co. - Bezeq. The Bezeq mobile laboratory allows measurement of electromagnetic field density and Bit Error Rate (BER) after Viterbi decoder. In addition, the equipment enables the observation of image quality including synchronization disturbances. A fairly straight section of road and free of heavy traffic was chosen for conducting experiments (see Figure 1)



Figure 1. Rout and transmitter (Tx) location for Doppler Effect influence checking.

Two sets of measurements were recorded for two discrete speeds: $V = 40\text{km/h}$ and $V = 120\text{km/h}$. The results of these experiments one can see on Figure 2. The number of synchronization losses increases proportionally according to the increase in vehicle speed due to the Doppler Effect

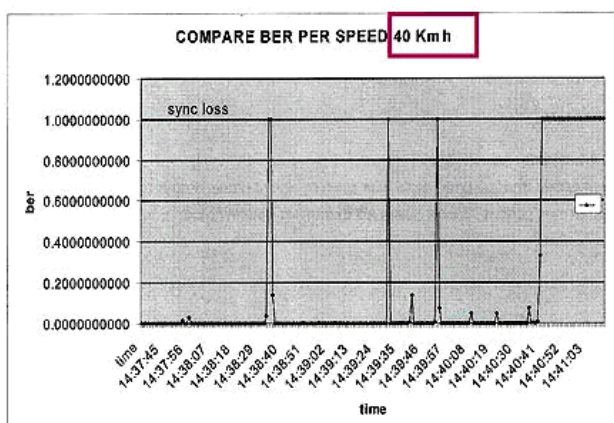


Figure 2a, Speed 40km/h

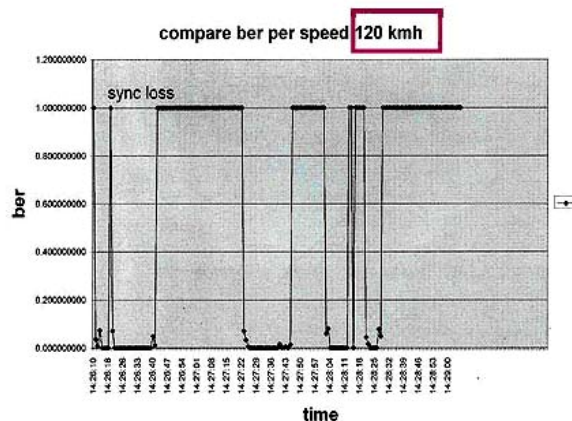


Figure 2b, Speed 120 km/h

Figures 2. Doppler Effect influence measurements

The enhanced OFDMA method, called the Frequency Bank Signal (FBS) method, is capable of mitigating the Doppler effects, and yield s high spectral efficiency by removing the need for pilot signals, and hence achieves higher throughputs. The basic principles of FBS have been published in [9]. In this paper we apply the FBS method to the HAP system, It is shown that using the FBS method the throughput of the HAP systems can be greatly enhanced in comparison with common OFDMA methods.

2. THE EFFECT OF DOPPLER SHIFT ON THE OFDM SIGNALS

In a multi-path channel the duration of a received symbol is subject to changes due to the variations in the length of the signal propagation path. The change of the signal duration will be denoted hereafter by factor k_d . However, since the frequency changes by the same factor k_d the number of carrier cycles in each symbol does not change, regardless of how fast the Transmitters (Tx) or Receivers (Rx) move. So in case of Doppler Shift, the frequency f and symbol time T are varied by a factor of k_d [2]

$$k_d = 1 + \frac{V}{c} \cos \varphi, \quad (1)$$

Where V is the moving object velocity, c is the light velocity and φ is the angle between the directions of signal propagation and the moving objects .Note that under these circumstances, the orthogonal condition prevails:

$$[(f_{i+1} - f_i) \cdot k_d] \cdot [T/k_d] = 1$$

In real situations, however, the orthogonal property of the subcarriers will be violated to some extent. Since the receiver's synchronization system cannot react instantly to changes in the symbol period or in the FFT parameters, we may assume that the Rx symbol time set by the symbol synchronization system remains at a fixed value. A Doppler shift of $\Delta\omega$ introduced an a phase shift of $\Delta\omega t$ in the received signal, and an additional phase shift due to incompatibility between carrier frequencies and the spectral components after FFT,

. Furthers influences include ICI (Inter-carrier interferences) due to partial loss of the orthogonal, changes of the pilot signals parameters,

and a time delay (or forestalling) between adjacent symbols due to incompatibility between of the received symbol duration and Rx clock synchronization system [1, 2].

Fig. 3 depicts an example of a typical HAP system using the OFDMA technology system [5,10] with symbol duration 0.1ms, frequency difference between carriers (ΔF) 10kHz, central frequency in the 2GHz L band range and from 5.85 to 7.075 GHz allocated by the ITU for the future HAPS. These higher frequency bands are required especially for broadband mobile radio, vehicles at speed of up to 300 km/h, and even more for aircrafts . The angle shift change as function of the distance between the HAP and the vehicle. ?

Using Equation. (1) the Doppler shift is estimated as ± 2.8 kHz or 30% of ΔF . It should be noted that also the reflected signals undergo a Doppler shift.

To mitigate the ill effects of a randomly changing Doppler frequency shift, OFDMA uses pilot signals, which leads to a significant increase in power, and system redundancy [9,10]. The HAP systems, on the other hand, are characterized by the favorable Rician distribution as the higher altitude and the resulting transmission angles produce a line of sight .This leads to a lower level of fading and Doppler effects. In addition, the higher operation ranges of a few hundreds km results in a significant reduction of hand over steps. For similar scenarios HAPS will be more

advantageous than Satellites due to their significantly less dispersion losses and lower cost .

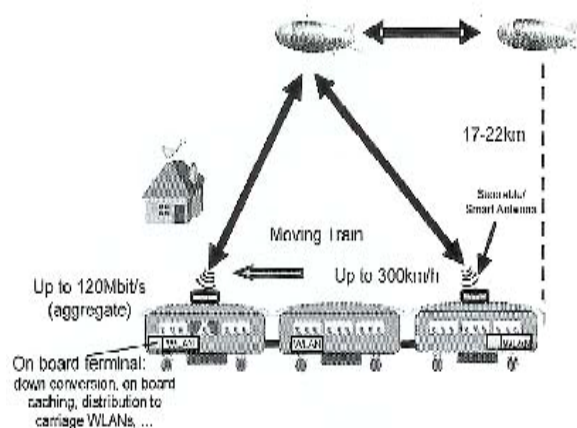


Figure 3. Scenario of the radio communication link between HAP and a mobile high speed train

We now proceed with the mathematical description of the OFDMA signal variations due to Doppler shift. The discrete Fourier transform (DFT) of $\{x_j\}_{j=0}^{N-1}$ is given by :

$$X_k = \sum_{j=0}^{N-1} x_j e^{-i \frac{2\pi}{N} kj}, \quad k = 0, \dots, N-1 \quad (2)$$

And the inverse discrete Fourier transform:

$$x_j = \frac{1}{N} \sum_{k=0}^{N-1} X_k e^{i \frac{2\pi}{N} kj}, \quad j = 0, \dots, N-1 \quad (3)$$

Here $x_j, \quad j = 0, \dots, N-1$ are N samples in time domain, and $X_k, \quad k = 0, \dots, N-1$ are N spectral components. Defining: $t_j = \frac{T}{N} j,$

$$\omega_k = \frac{2\pi}{T} k, \quad \text{Eq.s (2) and (3) can be rewritten}$$

as

$$X_k = X(\omega_k) = \sum_{j=0}^{N-1} x(t_j) e^{-i\omega_k t_j}, \quad (4)$$

$$k = 0, \dots, N-1$$

$$x_j = x(t_j) = \frac{1}{N} \sum_{k=0}^{N-1} X(\omega_k) e^{i\omega_k t_j}, \quad (5)$$

$$j = 0, \dots, N-1$$

In general, X_k is a complex number whose absolute value $|X_k|$ and angle $\angle X_k$ are the amplitude and phase of the k^{th} frequency

component. Since $\{x_j\}_{j=0}^{N-1}$ is a real signal, its DFT is symmetric, i.e. $X_{N-k} = X_k^*$ (where X_k^* denotes the complex conjugate of X_k).

As stated above, the Doppler shift leads to spectrum variations [9,11].

Due to the Doppler frequency shifts, the frequency of each component is shifted to

$$\tilde{\omega}_k = \omega_k + \Delta\omega_k, \quad \text{where } \Delta\omega_k = \frac{2\pi}{T}\delta_k$$

and δ_k denotes the relative shift of the k^{th} component. In the time domain the new signal

$$\begin{aligned} \tilde{x}_j &= \tilde{x}(t_j) = \frac{1}{N} \sum_{k=0}^{N-1} X(\omega_k) e^{i\tilde{\omega}_k t_j} \\ &= \frac{1}{N} \sum_{k=0}^{N-1} X(\omega_k) e^{i(\omega_k + \Delta\omega_k) t_j} \\ &= \frac{1}{N} \sum_{k=0}^{N-1} X_k e^{i\frac{2\pi}{N}(k+\delta_k)j} \\ &= \frac{1}{N} \sum_{m=0}^{N-1} X_m e^{i\frac{2\pi}{N}(m+\delta_m)j} \end{aligned} \quad (6)$$

since $\{\tilde{x}_j\}_{j=0}^{N-1}$ is a real signal,

$$\Delta\omega_{N-k} = -\Delta\omega_k, \text{ i.e. } \delta_{N-k} = -\delta_k.$$

The spectrum of the new signal is

$$\begin{aligned} \tilde{X}_k &= \sum_{j=0}^{N-1} \tilde{x}_j e^{-\frac{2\pi i}{N}kj} \\ &= \sum_{j=0}^{N-1} \left(\frac{1}{N} \sum_{m=0}^{N-1} X_m e^{i\frac{2\pi}{N}(m+\delta_m)j} \right) e^{-\frac{2\pi i}{N}kj} \\ &= \sum_{m=0}^{N-1} X_m \sum_{j=0}^{N-1} \frac{1}{N} e^{i\frac{2\pi}{N}(m+\delta_m)j} e^{-\frac{2\pi i}{N}kj} \\ &= \sum_{m=0}^{N-1} X_m \frac{1}{N} \sum_{j=0}^{N-1} e^{i\frac{2\pi}{N}(m+\delta_m-k)j} \end{aligned}$$

Therefore

$$\tilde{X}_k = \sum_{m=0}^{N-1} a_{km}(\delta_m) X_m \quad (7)$$

Where

$$a_{km}(\delta_m) = \frac{1}{N} \sum_{j=0}^{N-1} e^{i\frac{2\pi}{N}(m+\delta_m-k)j} \quad (8)$$

In other words, we can obtain the new spectrum vector \tilde{X} of length N by multiplying the $N \times N$ matrix a by the original spectrum vector X of length N . Matrix element $a_{km}(\delta_m)$ shows how the original m^{th} spectral component affects the new k^{th} spectral component. The matrix elements can be computed using Eq. (8).

If $\delta_m = 0$, then

$$a_{km}(0) = \begin{cases} 1, & k = m \\ 0, & k \neq m \end{cases} \quad (9.1)$$

For small $\delta_m \neq 0$ ($0 < |\delta_m| < 1$), using

$$\sum_{j=0}^{N-1} q^j = \frac{1-q^N}{1-q}, \quad q \neq 1,$$

for $q = e^{i\frac{2\pi}{N}(m+\delta_m-k)}$, we obtain

$$\begin{aligned} a_{k,m}(\delta_m) &= \frac{1}{N} \sum_{j=0}^{N-1} e^{i\frac{2\pi}{N}(m+\delta_m-k)j} \\ &= \frac{1}{N} \cdot \frac{1 - e^{i2\pi(m+\delta_m-k)}}{1 - e^{i\frac{2\pi}{N}(m+\delta_m-k)}} \\ &= \frac{1}{N} \cdot \frac{1 - e^{i2\pi\delta_m}}{1 - e^{i\frac{2\pi}{N}(m+\delta_m-k)}} \\ &= \frac{1}{N} \cdot \frac{1 - e^{i2\pi(m+\delta_m-k)}}{1 - e^{i\frac{2\pi}{N}(m+\delta_m-k)}} \\ &= \frac{1}{N} \cdot \frac{1 - e^{i2\pi\delta_m}}{1 - e^{i\frac{2\pi}{N}(m+\delta_m-k)}} \end{aligned} \quad (9.2)$$

$\{a_{k,m}(\delta_j)\}_{k,m=0}^{N-1}$ is a $N \times N$ matrix whose entries are complex numbers depending on $\{\delta_m\}_{m=0}^{N-1}$. If $\delta_m = 0$ for all $m = 0, \dots, N-1$, then (9.1) implies that

$\{a_{k,m}(\delta_m)\}_{k,m=0}^{N-1}$ is the identity $N \times N$ matrix

and in this case $\tilde{X}_k = X_k$ for all

$k = 0, \dots, N - 1$. In other words, if there are no frequency shifts, then the spectrum is not changed, as expected [8].

The relation $\delta_{N-k} = -\delta_k$ implies

$$a_{N-k, N-m}(\delta_{N-m}) = (a_{k,m}(\delta_m))^*$$

Note that the spectral components affected by the Doppler effect can be computed by Eq.s (7), (8). Remarkably, these numerical simulation and calculations do not require FFT size increasing. We believe that this can be a significant contribution to simulation design.

3. The FBS-1 METHOD

FBS combines the OFDMA principles with the phase shift compensation used in the PAL-TV systems, and spread spectrum concept using Walsh functions based on the Walsh-Hadamard matrix. In PAL-TV systems, prior to transmitting a color signal, the system's phase sign is changed every second line. In decoders, the phase sign is returned and summed together with phases of neighboring lines. As a result, phase deviations in the channel φ are compensated for [9].

In the first version of the FBS method (FBS-1) [9,10], an OFDMA system with eight single-carrier MPSK modulation signals is transformed to an FBS-1 system with the same eight signals on the same eight carriers (see Fig4). In this method, each signal phase is transmitted eight times with a varying phase sign corresponding to one of the eight Walsh-Hadamard matrix rows.

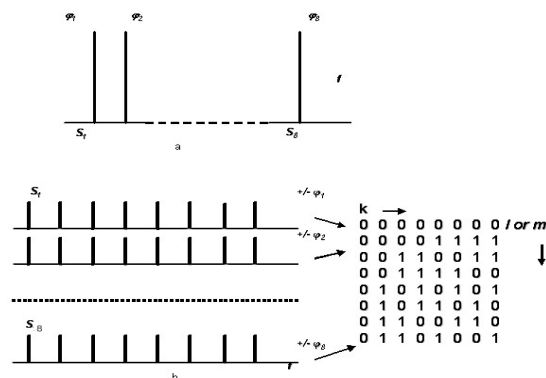


Figure 4. Transition from OFDMA (a) to FBS-1 (b)

For transmitting N signals on N carriers, the FBS signals are:

$$S_{(kl), FBS-1} = E_l \sum_{k=0}^{N-1} e^{j[2\pi f_k t + (-1)^{W_{kl}} (\theta_l + \beta_l)]}, \quad (10)$$

where

E_l - component magnitude, $l = 0, \dots, N - 1$ or Walsh-Hadamard matrix lines

θ_l - initial phase, chosen for a certain signal. For example, it is either 45° or other

β_l - information symbol of the l^{th} FBS signal (BPSK or QPSK representation),

$f_k = f_0 + k\Delta f$ - FBS carrier frequencies, $k = 0, \dots, N - 1$ or Walsh-Hadamard matrix columns

W_{kl} - sequence of phases of the l^{th} FBS carrier pattern.

To receive one of these signals, for example signal number 2, the following algorithm must be implemented: the S_2 receiver receives all signals together, makes FFT, obtains eight spectral components (amplitudes and phases), changes the phase signs of components 5, 6, 7 and 8 (corresponding to the second row of the Walsh-Hadamard matrix in Fig.2.). The result will be equal to the phase sum divided by eight. The phase sum of the other seven signals should be equal to zero [9].

We calculate arithmetical (not vector) sum φ_k of all signals on each carrier and use amplitude corresponding to:

Fig. 5 illustrate the main advantage of using the FBS-1 method.

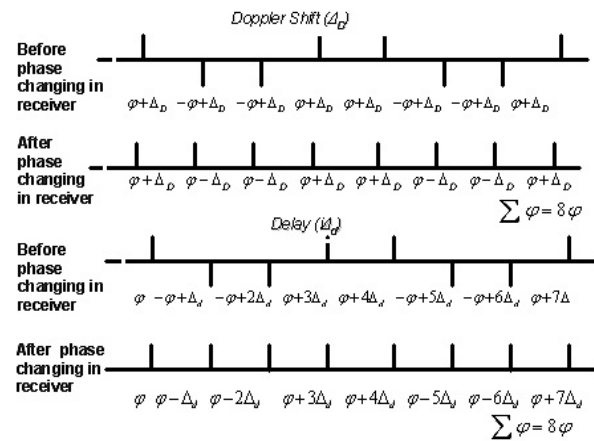


Figure 5. Phase shift compensation after decoding FBS-1

In the case of symmetrical Walsh functions, for example, 0 1 1 0 0 1 1 0, the Doppler Shift and Delay have no influence on FBS-1

reception. One can see that in Fig. 5 when phase shift due to delay is proportional to frequency. If the Walsh function is nonsymmetrical, (for example 0 0 1 1 0 0 1 1), there will be an additional phase shift, which is independent of the phase information and can be compensated for.

4. The FBS-2 METHOD

During the phase compensation process of the FBS-1 method, there is usually a certain level of data loss in the amplitude. Therefore, it is possible to implement only phase modulations e.g. MPSK [9,10]. To overcome these difficulties we present the FBS-2 system [11,12]. In this upgraded version, one can implement other modulation methods, such as MQAM. For transmitting N/2 sub-signals in the FBS-2 system we use N orthogonal sub-carriers f_1, f_2, \dots, f_m and Walsh-Hadamard matrix of order N. For each symbol of each sub-signal:

$$A = \sqrt{I^2 + Q^2}, \quad \varphi = \arctg \frac{I}{Q}$$

we present I and Q components

$$I = A \sin \varphi \quad \text{and} \quad Q = A \cos \varphi \quad \text{and}$$

$$A_m, \quad 2\pi m \leq \varphi_k < 2\pi(m+1)$$

The I and Q values are transmitted separately on N sub-carriers correspond to one of the pairs of Walsh functions selected from an N×N Walsh-Hadamard matrix. For example, in the case of N = 8, using the pair:

0 1 1 0 1 0 0 1
0 1 0 1 0 1 0 1

the following I and Q values are transmitted:

I -I -I I -I I I -I
Q -Q Q -Q Q -Q Q -Q

When receiving a transmitted sub-signal, it is necessary to implement the opposite process with the help of the same pair of Walsh functions. The sum of all values in the first line is 8I and the sum of all values in the second line is 8Q. By knowing the values for I and Q, we can find A and φ .

The I and Q sums of the other signals will be equal to zero.

Each selected pair of Walsh functions may be added to make a symmetric form. For example, the four pairs of Walsh functions listed in Table 1 give a symmetrical form.

Table 1.; Walsh functions choosing examples

for getting a symmetrical form.

	First couple	Second couple	Third couple	Fourth couple
I	0 1 1 0 1 0 0 1	0 0 1 1 1 1 0 0	0 0 0 0 1 1 1 1	0 1 1 0 0 1 1 0
Q	0 1 0 1 0 1 0 1	0 1 0 1 1 0 1 0	0 0 1 1 0 0 1 1	0 0 0 0 0 0 0 0
	+ + + +	+ . . + + . . +	+ + + +	+ . . + + . . +

One of the FBS-2 signals with row l for I and row m of the Walsh-Hadamard matrix for Q, can be presented as follows [12]

$$s_{(l,m),FBS-2} = E_{l,m} \sum_{k=1}^N \left\{ \begin{aligned} & \left[\sin[2\pi f_k + (-1)^{W_{kl}}(\theta_{l,m} + \beta_{l,m})] + \right. \\ & \left. + \cos[2\pi f_k + (-1)^{W_{km}}(\theta_{l,m} + \beta_{l,m})] \right] \end{aligned} \right\} \quad (11)$$

For comparison purposes, we shall use a typical FBS-2 system, that uses N carriers for transmitting N signals. Since FBS-2 utilizes only the I and Q carriers, N/2 signals may be transmitted on the same allocated channels. Nevertheless, the QAM modulation technique (used in FBS-2) allows transmitting twice as much data as the PSK modulation technique (used in FBS-1), for the same allocated channels.

It is well known that signal to noise ratio (SNR) for transmitting signal using 16QAM should be greater by at least 4dB than the corresponding ratio using QPSK with the same BER. In the case of FBS-2, the required SNR for 16QAM should be only by 2.7 dB relative to QPSK. This is due to the fact that in FBS-2, M signals are summed up coherently, but M uncorrelated noise components are summed in the sense of energies. However if we take into consideration PS influence in OFDMA, we will see that the SNRs in OFDM and in FBS-2 are approximately equal.

5. SIMULATION RESULTS

A typical mobile communication system consisting of a HAP and various cellular combinations, was implemented in order to make a comparative study between OFDMA and the FBS systems [11,12]. We consider a system with four receivers and symbol duration of $T = 100 \mu s$, such that, the frequency difference between sub carriers will be $\Delta F = 1/T = 10 \text{ kHz}$. We assume the Doppler shift is 3% of ΔF , and the phase shift per each symbol time due to delay 3.9° . Four signals are transmitted. In case of OFDMA, each symbol is transmitted on two sub-carriers using QPSK,

and in case of FBS-2 on eight sub-carriers using 16QAM.

Simulation results are shown in Fig. 6 (OFDMA) and Fig. 7 (FBS-2). In the case of OFDMA with pilot ratio of 1:10 (upper curves in Fig.4) the resulting BER is $\sim 10^{-1}$ is in the range of uncorrectable error floor. Acceptable BERs ($5 \cdot 10^{-3}$) are obtained only by increasing the pilot ratio up to 1:2. Taking into account the 3 dB higher powers of the pilots, the resulting redundancy is more than 100%.

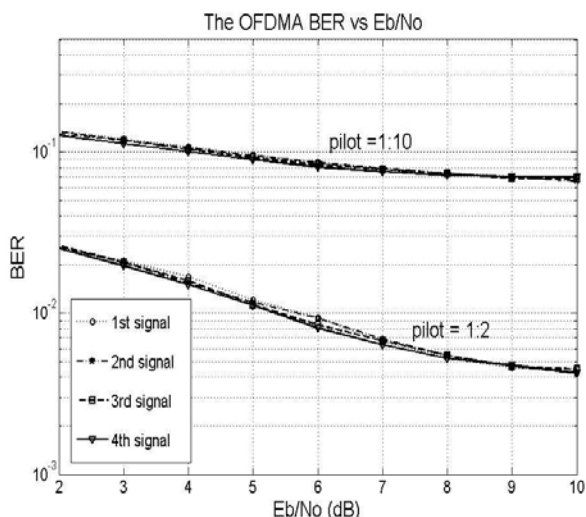


Fig. 6. BER calculations in case of OFDMA for different numbers of pilot signals

Fig. 7 shows the simulation results for the case of the FBS-2 method on the conditions like on Fig. 6. It is seen that in this case the BER is not affected by phase distortions due to the Doppler Effect. The relatively higher values of the fourth signal are attributed to the fact that for this signal the all zero Walsh function W_0 was applied.

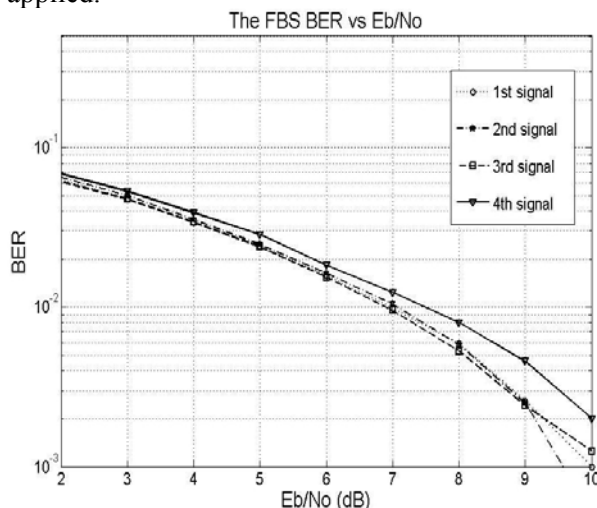


Fig. 7. BER calculations in case of FBS-2 with no pilot signals

Two main restrictions exist equally for both FBS and FDMA system design: $T > \tau_{\max}$ and $\Delta F \times N < B_c$.

Where B_c is the coherence bandwidth [1].

6. CONCLUSIONS

A future HAP broadband mobile radio system based on the FBS method is presented for high speed vehicles., and compared to OFDMA based HAP systems..

It is shown in this paper that the FBS-HAP system allows transmission of the same quantity of information on the same frequency band and with the same power, as the OFDMA-HAP system.

. The main FBS advantages are:

- A significant decrease of the Doppler frequency shift effects, as well as the time delays and multi-paths influences.
- FBS removes the need for conducting tests or using pilot signals and/or equalizing processesng prolonged selective fading by means of randomly shifting sub-carriers frequencies.
- The FBS method can be implemented in different wireless communication systems including HAPS using various modulation techniques.[3,8]
- FBS allows for improving the radio performances and quality of HAPS even in broadband communication with very high speed vehicles [4, 10] All these advantages are achieved without any extra cost in frequency band and without an increase in the system power supply. Implementation of the FBS system will result in a significant increase in the HAP throughput affording very fast internet communication also for fast TGV or airplane passengers.

1. References

2. J. Gavan, S.Tapuchi and D. Grace "Concepts and Main Applications of High Altitude Platforms Radio Relays" The Radio Science Bulletin. N. 330 September 2009.pp(20-31)
3. J. Gavan and S. Tapuchi, "Low Interference Wideband Wireless Systems Using High Altitude Platforms," Invited Paper, URSI General Assembly ,Chicago., August 2008, pp.(1-4).
4. R. van Nee, and R. Prasad, . OFDM for wireless

- multimedia communications, Artech House, 2000.
5. C. W. Lee, Mobile cellular telecommunications systems, McGraw-Hill, Inc., 1989.
 6. R. Struzak, Mobile telecommunications via stratosphere, Intercoms international communication project, 2003, pp(1-20).
 7. Grace and M. H. Capstick, Integrating Users into the Wider Broadband Network via High Altitude Platforms, IEEE Wireless Communications, October 2005.
 8. S.G.M. Djuknic, J. Freidenfelds and Y. Okunev, Establishing Wireless Communications Services via High-Altitude Aeronautical Platforms: A Concept Whose Time Has Come?, IEEE Commun. Mag., pp.(128-135), Sept., 1997.
 9. D. Grace, C. Spillard, T. C. Tozer, High Altitude Platform Resource Management Strategies with Improved Connection Admission Control, IEEE Wireless Personal Mobile Conference, October, 2003. pp.
 10. T.C Tozer, D. Grace, High altitude platforms for wireless communication, Electronics & communication engineering journal. June 2001 pp (127-137).
 11. J. Gavan, M. Haridim, Stratospheric Quasi-Stationary Platforms (SQSP) Can they Replace Communication Satellite Systems, Telecommunications and Space Journal. Volume 4 1997, pp(275-288)
 12. M. Bank, On increasing OFDM method frequency efficiency opportunity, IEEE Transactions on Broadcasting, 50(2), 2004 pp (165-171).
 13. www.OFDMA-Manfred.com
 14. ITU-R working document 5C/76-E Interference analysis modeling for sharing between HAPS gateway links in the range 5 850-7 075 MHz and other services 20.10.08

Short biography:

Michael Bank received the BA and M.Sc. degrees in communicational engineering from the Leningrad Institute of Communications in 1960, received the Ph.D. degree in 1969 in the field of FM signal detection. He received Doctor of Science degree (Russian equivalent of professor) in 1990. Since 1992 he is a consultant of Israel communicational company Bezeq and a lecturer in the Holon Academic Institute of Technology. His research interests include digital modulation, digital signal processing and RF receiving theory.

Saad Tapuchi earned the B.Sc. degree from the Ben-Gurion University of the Negev, Beer-Sheva 1973, the M.Sc. from the Hebrew University of Jerusalem – School of Applied Science and Technology 1982 and Ph.D. from Ben-Gurion University of the Negev, Beer-Sheva 1988.

Dr. Saad Tapuchi served as the Head of the Telecommunication department in the Telecommunication school for practical engineering of the Bezek Corporation in Jerusalem from 1973 to 1986. In 1986 he was nominated as director of the Telecommunication School till 1998. From 1998 Dr. Saad Tapuchi began working at Sami Shamoon College of engineering at two campuses in Beer-Sheva & Ashdod. Since 2002 he was elected as Dean of the EEC Faculty of the Sami Shamoon College of engineering.

Motti Haridim received his M.Sc. degree in electrical engineering from the University of Washington in 1986 and the Ph.D. degree in electrical engineering from Technion of Israel in 1992. Since 1994 he has joined Holon Institute of Technology (HIT). During 2002-2008 Prof. Haridim was the head of the Dept. of Communication Engineering at HIT. His research activities focus mainly on the physical layer of communication systems, including optical systems, microwave photonics, RF communications, and antennas. He has published over 60 papers. Prof. Haridim acts as a consultant in RF communication systems and antennas to several large Israeli companies.

Miriam Bank, Ph.D. in mathematics (Hebrew University of Jerusalem). Interests: applied mathematics, including spectral transform methods, partial differential equations. Lecturer in the Hebrew University and in Jerusalem College of Engineering.

Jacob Gavan, was elected as IEEE fellow in 1995 and founded a department of Communication Engineering at the Holon Institute of Technology (HIT) in Israel. He was selected as Dean of the HIT faculty of Engineering and as Full Professor from December 2001. Now Jacob is head of a new communication engineering department in the SAMI Shamoon College of Engineering (SCE). Jacob has published over 150 papers on theoretical and Applied EMC, Satellite Communications, and Radar Systems. Professor Jacob Gavan is active in IEEE as ex associated editor of the Trans. on EMC and DL of the Communication society. In URSI Jacob is cochairman of E8 working group on "Electromagnetic Compatibility in Wire and Wireless Communication Systems" and of the SPS committee. From 2008 he served as RSB guest editor on a special issue on High Altitude Platforms (HAPS). Jacob earned the best paper award from the IEEE International Symposium on EMC in two international conferences.

Boris Hill earned the M.Sc. degree in computer engineering from the Polytechnic Institute of Riga in 1970. Since 1999 he is a system engineer in the Ness Ltd. Interests in research of frequency affiliation problem and Communication networks design